ChemComm

Accepted Manuscript

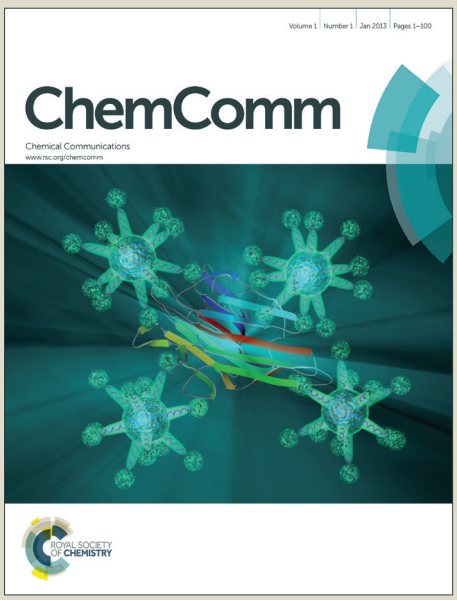

ROYAL SOCIETY OF CHEMISTRY

www.rsc.org/chemcomm

Journal Name

RSCPublishing

COMMUNICATION

Enhanced photocatalytic water oxidation efficiency with $Ni(OH)_2$ catalysts deposited on α-Fe_2O_3 via ALD

Cite this: DOI: 10.1039/x0xx00000x

Kelley M. H. Young and Thomas W. Hamann*

Received 00th January 2012,
Accepted 00th January 2012

DOI: 10.1039/x0xx00000x

www.rsc.org/

Atomic layer deposition was used to deposit NiO onto thin-film α-Fe_2O_3 electrodes for photocatalytic water splitting. Photoelectrochemical conditioning of the deposited NiO converts it to $Ni(OH)_2$, which results in a stable reduction of the photocurrent onset potential for water oxidation by ~300 mV and improves photocurrent density by two-fold at 1.23V vs RHE as compared to untreated α-Fe_2O_3. This enhanced performance is shown to be due to improved charge separation with the ion-permeable $Ni(OH)_2$ catalyst film. These results not only demonstrate one of the most effective water oxidation catalysts when integrated with hematite, but help establish the operational principles that lead to the improved performance.

The development of materials capable of converting solar energy to chemical fuels is of great interest since this process offers the possibility of reducing our dependence on carbon based fuels.[1–3] One method to generate solar fuels is to use a semiconductor to split water and produce O_2 and the useable fuel H_2. Ideally, the generation of H_2 and O_2 could be performed on separate photoelectrodes allowing for independent photocathode (H_2 generation) and photoanode (O_2 generation) optimization. One of the most promising photoanode materials for water oxidation is hematite (α-Fe_2O_3), which has desirable material characteristics, such as high elemental abundance, good light absorption into the visible region, stability in neutral and basic aqueous solutions, and a favourable valence band position to facilitate water oxidation.[4] However, hematite suffers from a short hole collection length compared to its light absorption depth and slow water oxidation kinetics at the surface, which limit its overall solar-to-fuel conversion efficiency.[5–16] In order to lower the activation barrier for water oxidation and reduce or bypass recombination of photogenerated holes, catalysts such as IrO_x, Co-Pi, $Co(OH)_2/Co_3O_4$, $Ni(OH)_2$, and $NiFeO_x$ have been added to hematite's surface.[17–24] While these catalysts have shown an improvement for the onset potential of water oxidation, cathodic shifts ranging from approximately 200-300 mV, some are unstable, are not deposited in a conformal manner or have competing light absorbance in the visible region which impedes the ability to be used effectively in a nanostructured device. In addition, there is a disagreement in the mechanism to which the improvement in water oxidation onset occurs.

$Ni(OH)_2$ is an especially interesting water oxidation catalyst as it is composed of earth abundant elements, has minimal competitive light absorption, is stable in neutral and basic solutions, and has shown good electrocatalytic activity for water oxidation.[25,26] Li and co-workers recently reported Fe_2O_3 nanowires coated with $Ni(OH)_2$ via dipcoating. This procedure resulted in an initial cathodic shift of the photocurrent density; however the photocurrent decayed by ~90% – to values lower than the bare hematite – over 30 seconds. This behaviour was attributed to fast oxidation of Ni^{2+} to Ni^{3+}, followed by a rate limiting step of further oxidation to a Ni^{4+} species, thus resulting in the NiOOH film storing charge but not producing a sustained enhancement of water oxidation.[17] $Ni(OH)_2$/NiOOH has recently been shown to produce a high-quality junction when paired with a TiO_2 single crystal semiconductor electrodes which resulted in excellent stable water oxidation performance compared to IrO_x.[26,27] This discrepancy in the effectiveness and behaviour of $Ni(OH)_2$ as a water oxidation catalyst on semiconductor surfaces, as well as a general effort to improve and understand semiconductor catalyst junctions, motivated this research.

Herein we report using atomic layer deposition (ALD) to deposit thin films of NiO onto the surface of planer Fe_2O_3 electrodes. ALD allows for self-limiting film growth which ensures reproducible conformal films with tuneable thickness. Since it is not a line-of-sight technique, these films can also be deposited uniformly on high surface area hematite films. Working electrodes consist of a 20 nm Fe_2O_3 (300 ALD cycles) film deposited on top of 2 nm Ga_2O_3 (18 ALD cycles) coated fluorine-doped tin oxide (FTO) substrate via ALD following a previously reported procedure.[16,28,29] An additional ~10 nm NiO (100 ALD cycles) film was deposited on some Fe_2O_3 electrodes via ALD using Nickel alkyl amidinate (Ni-amd) and H_2O as the precursors following a modified procedure as described in supporting information.[30] The NiO-coated hematite was annealed and then stored at 80°C when not in use, which we found to be critical to achieve reproducible results. Electrochemical measurements were performed using a custom glass 3-electrode cell with a Pt mesh counter electrode, homemade Ag/AgCl reference electrode, and a bare Fe_2O_3 or NiO-coated Fe_2O_3 working electrode clamped to the cell. All cells were measured in pH 14 and were illuminated through the solution side with a xenon arc lamp fitted with an A.M. 1.5 filter under 1 sun (100 $mWcm^{-2}$) conditions. Six sets of electrodes were fabricated and measured, with good

reproducibility across all sets. See supporting information for detailed electrode preparation and experimental procedures.

Current density vs. applied voltage (*J-V*) measurements of bare and NiO-coated Fe_2O_3 electrodes were performed in the dark and under illumination. Figure 1 shows a typical *J-V* curve under 1 sun illumination (black curve) of bare Fe_2O_3 electrodes with a photocurrent onset of ~1.1 V vs RHE. Plots of dark currents are provided in supporting information (Fig S1). Electrodes with freshly annealed NiO-coated films, shown by the red curve in Figure 1, exhibit a small cathodic shift in the photocurrent onset and a small decrease in saturated photocurrent as compared to bare Fe_2O_3. Results of UV-vis measurements (Fig S2) show a negligible change in absorptance due to the addition of NiO; thus differences in light absorption cannot account for the change in *J-V* behaviour.

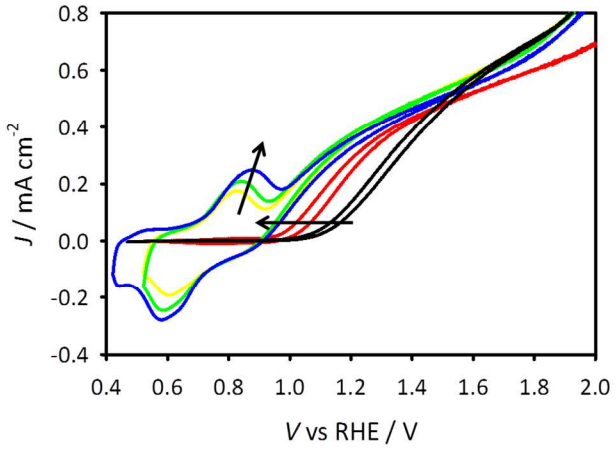

Figure 1. Plots of *J-V* curves for bare Fe_2O_3 (black) and NiO-coated Fe_2O_3 electrodes for as-deposited (red), and following 1 hour (yellow), 2 hours (green), and 3 hours (blue) of conditioning at 1.42 V vs RHE under 1 sun illumination.

The Boettcher group recently reported a conditioning procedure in which an anodic current density of 10 $mAcm^{-2}$ was applied for 6 hours to NiO_x electrocatalysts prepared by spin-coating.[26] Their Initial cyclic voltammetry (CV) scans showed a slight redox wave, but subsequent CV scans taken at 1 hour intervals indicated an increase in the redox wave attributed to the $NiOOH/Ni(OH)_2$ redox couple; a concomitant cathodic shift in the oxygen evolution reaction (OER) was observed. It was determined that NiOx underwent a structural change following electrochemical conditioning in which NiOx transforms from a rock salt to a layered, ion-permeable hydroxide/oxyhydroxide structure. The resulting NiOOH structure in these studies was determined to be the active catalyst for the OER.[26] We therefore adapted a similar conditioning procedure in which NiO-coated Fe_2O_3 electrodes were held at a constant voltage of 1.42 vs RHE under illumination for 1 hour increments. After one hour of conditioning there was an additional 100 mV cathodic shift (Figure 1, yellow) in the photocurrent onset potential as compared to the initial scan (red). In addition, a redox wave developed, which can be attributed to the Ni^{3+}/Ni^{2+} redox reaction.[26] Successive hours of conditioning were performed to monitor the electrode evolution, indicated by the arrows in Figure 1. In addition to the magnitude of the onset shift, the redox wave continued to increase with conditioning. This result correlates the increased magnitude of the $Ni^{3+/2+}$ redox wave with an apparent cathodic shift in the photocurrent onset. This correlation of improved photocurrent onset is likely due to the increased number of available Ni^{3+} sites as the film becomes more ion-permeable during conditioning, as shown in previous studies and discussed below.[26] This procedure was repeated for three hours at which point no change in the redox wave or *J-V* was observed. All electrodes used for photoelectrochemical measurements were therefore conditioned by this method for 3 hours.

X-ray photoelectron spectroscopy (XPS) measurements were performed on NiO-coated Fe_2O_3 before and after photo-electrochemical measurements to determine the nature of any structural change during the conditioning process (Fig S3). The Ni $2p_{3/2}$ peak was fitted using relative peak positions for both Ni^{2+} and Ni^{3+} oxides, which did not allow unambiguous identification of the oxidation state. The spectra are nominally identical for all samples, however, and are consistent with either NiO or $Ni(OH)_2$.[33,34] Fits of the O 1s peaks are more informative and indicate that as-deposited and annealed films are comprised of NiO, which is consistent with previous reports of the ALD of NiO under similar conditions.[30] The O 1s peaks changed upon conditioning; OH^- is the primary component for the O 1s peaks in the conditioned films, although some O^{2-} is still evident.[31] The conditioned films are therefore composed primarily of $Ni(OH)_2$, with a small fraction of NiO and/or NiOOH. Thus, we attribute the conditioning process to the structural change from cubic NiO to the layered $Ni(OH)_2$, a well known ion-permeable water oxidation catalyst. The redox wave that develops in the *J-V* curves shown in figure 1 is therefore attributed to the $NiOOH/Ni(OH)_2$ redox couple.

The photocurrent onset for bare Fe_2O_3 is approximately 1.1 V vs RHE with a photocurrent density of ~0.18 mA cm^{-2} at 1.23 V vs RHE. The addition of a conditioned $Ni(OH)_2$ film on Fe_2O_3 produces a cathodic shift of the photocurrent onset potential, although the precise magnitude cannot be accurately determined since the large $NiOOH/Ni(OH)_2$ capacitive redox wave obscures the Faradaic current voltage behaviour. In order to separate the capacitive and Faradaic currents and indentify the true onset potential, anodic current transients were measured. Figure 2a shows the current response to turning on the light at a constant potential of 1.17 V vs RHE. For the bare hematite electrode, there is a short spike of photocurrent which is attributed to trapping of photogenerated holes in surfaces states, which quickly decays to a very low steady state photocurrent density.[15] The $Ni(OH)_2$-coated Fe_2O_3 electrodes also exhibited an initial spike, however in this case it was followed by a relatively slow (4 second) multi-exponential decay to a steady-state Faradaic current. The photocurrent measured over the last 170 seconds was averaged to determine the steady state Faradaic photocurrent. Analogous measurements were performed at varying applied potentials and are shown as open symbols superimposed on the *J-V* scans in Figure 2b. From this, it can be seen that the photocurrent onset for $Ni(OH)_2$-coated Fe_2O_3 is indicated by the forward sweep of the *J-V* at approximately 800 mV vs RHE, which represents an approximately 300 mV cathodic shift for the photocurrent onset as compared to bare Fe_2O_3. We note that similar catalyst charging behaviour was observed for Co-Pi on hematite, however the resulting cathodic shift of the *J-V* curve was lower with a photocurrent onset of ~1 V vs RHE.[19] We further note that a previous report $Ni(OH)_2$-coated Fe_2O_3 indicated instability of the catalyst, with photocurrents dropping to very low values over 30 seconds.[17] For these measurements, once a plateau current was reached, the performance did not diminish rapidly; there is however, a slight decrease in photocurrent density over time, which is due to bubbles forming on the photoanode active area. When electrodes are cleared of bubbles and measured again, the original photocurrent is observed, indicating no degradation of electrode performance. We tentatively assign the greatly improved stability demonstrated here, compared to previous reports, to the $Ni(OH)_2$ deposition method,

however more work is required to confirm this. The steady state photocurrent is approximately 0.4 mA cm^{-2} at 1.23V vs RHE, which is more than double that of the bare electrode.

Cathodic current transients were also measured in response to turning off the light at several applied potentials. Figure 2c shows cathodic transient currents measured at potentials negative of the photocurrent onset, 1.05 V and 0.80 V vs RHE for bare (black trace) and $Ni(OH)_2$-coated Fe_2O_3 (red trace), respectively. For the bare Fe_2O_3 electrode, the transient spike is attributed to the de-trapping of holes, or the reduction of surface states.[15] The cathodic transient for $Ni(OH)_2$-coated Fe_2O_3, however, is attributed to the reduction of Ni^{3+} back to Ni^{2+}. This cathodic transient has an initial spike slightly larger than untreated Fe_2O_3 and takes a much longer time to decay back to essentially zero current density, indicating a greater amount of charge passed. This difference can be quantified by integrating the current transients. This integration produced a charge passed of approximately 1.6 $x10^{14}$ electrons per cm^2 for bare Fe_2O_3 electrodes and 1.6 x 10^{16} electrons per cm^2 passed for $Ni(OH)_2$-coated Fe_2O_3 electrodes. Assuming just the 0001 crystal face is exposed, the total density of iron atoms at the surface is 3.9 $x10^{14}$ cm^{-2}, thus 1.6 $x10^{14}$ cm^{-2} is consistent with a surface species. One hundred times more charge is stored in the 10 nm $Ni(OH)_2$ film; this indicates that the $Ni(OH)_2$-coated Fe_2O_3 must become ion-permeable to allow charge compensating ions to intercalate to the active $Ni^{3+/2+}$ sites, consistent with the large redox wave in the *J-V* curves.

Conclusions

We have shown that using by using ALD we were able to deposit thin films of NiO onto Fe_2O_3 photoelectrodes. XPS measurements indicated that freshly annealed NiO resulted in a slight improvement in the water oxidation *J-V* response in comparison to bare Fe_2O_3 electrodes. Photoelectrochemical conditioning of the NiO films produced a structural change to a layered $Ni(OH)_2$, as determined by XPS measurements. The structural change was monitored through the growth of a large $NiOOH/Ni(OH)_2$ redox wave in conjunction with further improvement in the water oxidation onset potential. The correlation of the increased stored charge (magnitude of redox wave in the *J-V* curve) upon conditioning with an the improvement of the *J-V* curve indicates that the primary attribute of the $Ni(OH)_2$ film is the ability to separate charge. This charge separation allows holes stored by $Ni(OH)_2$, as NiOOH, to oxidize water competitively with recombination with conduction band electrons. This behaviour is consistent with previous results of Co-Pi on Fe_2O_3 and $Ni(OH)_2$ on TiO_2 electrodes.[19,20,27] These results provide important insight into the design of water oxidation catalysts in contact with semiconductor electrodes. The most important parameter appears to be ion-permeability which allows charge separation, rather than intrinsically faster water oxidation kinetics of an electrocatalyst. Finally, the results reported herein are in contrast to previous reports of $Ni(OH)_2$ on Fe_2O_3, however the cause of this discrepancy is still not clear. Further investigations are ongoing in our lab in order to better understand the mechanistic details of these exciting results.

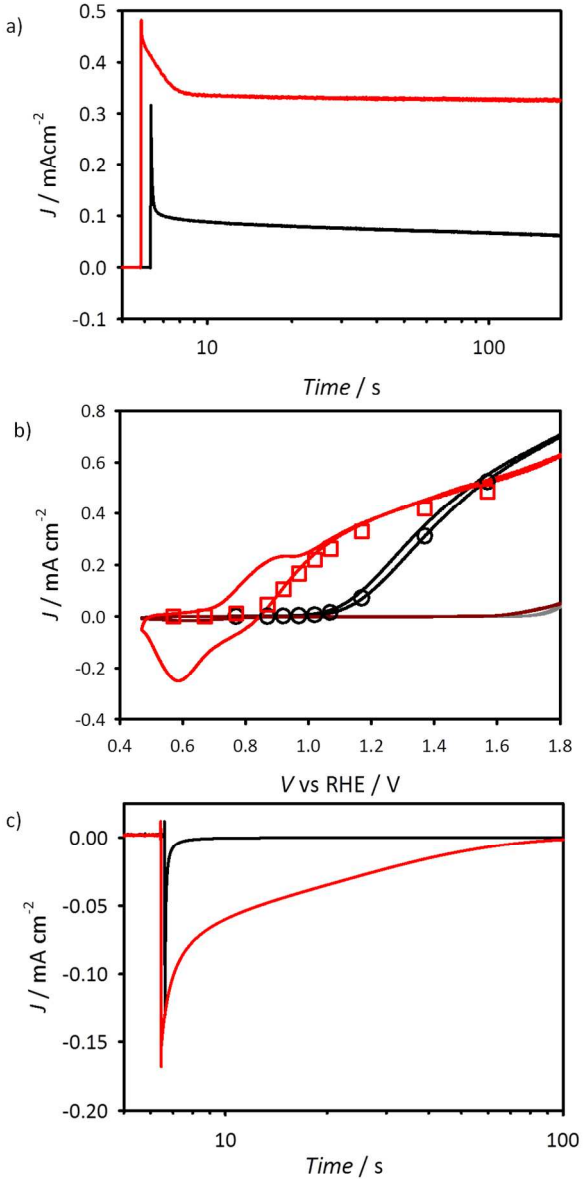

Figure 2. Bare Fe_2O_3 (black) and $Ni(OH)_2$-coated Fe_2O_3 (red) a) anodic (light on) current transient measurements at 1.17 V vs RHE, b) *J-V* plots under illumination and in the dark with superimposed steady-state Faradaic photocurrent measurements (open symbols), and c) cathodic (light off) current transient measurements for bare Fe_2O_3 (black) and $Ni(OH)_2$-coated Fe_2O_3 (red) at 1.05 and 0.800 V vs RHE, respectively.

Acknowledgements

TWH is grateful to the National Science Foundation (CHE-1150378) for support of this research.

Notes and references

Department of Chemistry, Michigan State University
578 South Shaw Lane
East Lansing, MI 48824 United States
E-Mail: hamann@chemistry.msu.edu

Electronic Supplementary Information (ESI) available: Detailed experimental procedures, plots of dark *J-V* curves and

absorptance measurements, and XPS results and analysis. See DOI: 10.1039/c000000x/

1. N. S. Lewis, *MRS Bull.*, 2007, **32**, 808–820.

2. G. W. Crabtree and N. S. Lewis, *Phys. Today*, 2007, **60**, 37–42.

3. N. S. Lewis and D. G. Nocera, *Proc. Natl. Acad. Sci.*, 2006, **103**, 15729–15735.

4. M. G. Walter, E. L. Warren, J. R. McKone, S. W. Boettcher, Q. Mi, E. a Santori, and N. S. Lewis, *Chem. Rev.*, 2010, **110**, 6446–73.

5. T. Lindgren, H. Wang, N. Beermann, L. Vayssieres, A. Hagfeldt, and S.-E. Lindquist, *Sol. Energy Mater. Sol. Cells*, 2002, **71**, 231–243.

6. U. Bjorksten, J. Moser, and M. Gratzel, *Chem. Mater.*, 1994, **6**, 858–863.

7. A. G. Joly, J. R. Williams, S. a. Chambers, G. Xiong, W. P. Hess, and D. M. Laman, *J. Appl. Phys.*, 2006, **99**, 053521.

8. B. M. Klahr and T. W. Hamann, *J. Phys. Chem. C*, 2011, **115**, 8393–8399.

9. T. W. Hamann, *Dalt. Trans.*, 2012, **41**, 7830–4.

10. C. Y. Cummings, F. Marken, L. M. Peter, A. a Tahir, and K. G. U. Wijayantha, *Chem. Commun.*, 2012, **48**, 2027–9.

11. K. G. Upul Wijayantha, S. Saremi-Yarahmadi, and L. M. Peter, *Phys. Chem. Chem. Phys.*, 2011, **13**, 5264–70.

12. C. Y. Cummings, F. Marken, L. M. Peter, K. G. U. Wijayantha, and A. A. Tahir, *J. Am. Chem. Soc.*, 2012, **134**, 1228–1234.

13. S. R. Pendlebury, A. J. Cowan, M. Barroso, K. Sivula, J. Ye, M. Grätzel, D. R. Klug, J. Tang, and J. R. Durrant, *Energy Environ. Sci.*, 2012, **5**, 6304.

14. A. J. Cowan, C. J. Barnett, S. R. Pendlebury, M. Barroso, K. Sivula, M. Grätzel, J. R. Durrant, and D. R. Klug, *J. Am. Chem. Soc.*, 2011, **133**, 10134–40.

15. B. Klahr, S. Gimenez, F. Fabregat-Santiago, J. Bisquert, and T. W. Hamann, *Energy Environ. Sci.*, 2012, **5**, 7626.

16. B. M. Klahr, A. B. F. Martinson, and T. W. Hamann, *Langmuir*, 2011, **27**, 461–8.

17. G. Wang, Y. Ling, X. Lu, T. Zhai, F. Qian, Y. Tong, and Y. Li, *Nanoscale*, 2013, **5**, 4129–33.

18. S. D. Tilley, M. Cornuz, K. Sivula, and M. Grätzel, *Angew. Chemie*, 2010, **122**, 6549–6552.

19. B. Klahr, S. Gimenez, F. Fabregat-santiago, J. Bisquert, and T. W. Hamann, *J. Am. Chem. Soc.*, 2012, **134**, 16693–16700.

20. D. K. Zhong and D. R. Gamelin, *J. Am. Chem. Soc.*, 2010, **132**, 4202–7.

21. C. Du, X. Yang, M. T. Mayer, H. Hoyt, J. Xie, G. McMahon, G. Bischoping, and D. Wang, *Angew. Chem. Int. Ed. Engl.*, 2013, **52**, 12692–5.

22. S. C. Riha, B. M. Klahr, E. C. Tyo, S. Seifert, S. Vajda, M. J. Pellin, T. W. Hamann, and A. B. F. Martinson, *ACS Nano*, 2013, **7**, 2396–2405.

23. J. Li, F. Meng, S. Suri, W. Ding, F. Huang, and N. Wu, *Chem. Commun. (Camb).*, 2012, **48**, 8213–5.

24. D. K. Bora, A. Braun, R. Erni, U. Müller, M. Döbeli, and E. C. Constable, *Phys. Chem. Chem. Phys.*, 2013, **15**, 12648–59.

25. J. M. Mckay and V. E. Henrich, *Phys. Rev. Lett.*, 1984, **53**, 2343–2346.

26. L. Trotochaud, J. K. Ranney, K. N. Williams, and S. W. Boettcher, *J. Am. Chem. Soc.*, 2012, **134**, 17253–61.

27. F. Lin and S. W. Boettcher, *Nat. Mater.*, 2014, **13**, 81–6.

28. T. Hisatomi, H. Dotan, M. Stefik, K. Sivula, A. Rothschild, M. Grätzel, and N. Mathews, *Adv. Mater.*, 2012, **24**, 2699–702.

29. O. Zandi, J. A. Beardslee, and T. W. Hamann, *Submitted*.

30. E. Thimsen, A. B. F. Martinson, J. W. Elam, and M. J. Pellin, *J. Phys. Chem. C*, 2012, **116**, 16830–16840.

31. B. P. Payne, M. C. Biesinger, and N. S. McIntyre, *J. Electron Spectros. Relat. Phenomena*, 2009, **175**, 55–65.